THE JOURNAL OF PHYSICAL CHEMISTRY B LETTERS

2006, *110,* 7609−7612
Published on Web 03/31/2006

Infrared Spectroscopic Characterization of [2]Rotaxane Molecular Switch Tunnel Junction Devices

Erica DeIonno,[†] Hsian-Rong Tseng,[‡] Desmond D. Harvey,[§] J. Fraser Stoddart,[‡] and James R. Heath*,[†]

Department of Chemistry, California Institute of Technology, 1200 East California Blvd, MC 127-72 Pasadena, California 91125, California NanoSystems Institute and Department of Chemistry and Biochemistry, University of California, Los Angeles, 405 Hilgard Ave, Los Angeles, California 90095-1569

Received: February 6, 2006; In Final Form: March 14, 2006

Langmuir−Blodgett monolayers of a bistable [2]rotaxane were prepared at packing densities of 118, 73, and 54 Å^2/molecule. The monolayers were both characterized via infrared spectroscopy before and after evaporation of a 2 nm film of titanium and incorporated into molecular switch tunnel junction devices. The study suggests that the evaporation process primarily affects portions of the molecule exposed to the metal atom source. Thus, in tightly packed monolayers (73 and 54 Å^2/molecule), only the portions of the [2]rotaxane that are present at the molecule/air interface are clearly affected, leaving key functionality necessary for switching intact. Monolayers transferred at a lower pressure (118 Å^2/molecule) exhibit nonspecific damage and poor switching behavior following Ti deposition. These results indicate that tightly packed monolayers and sacrificial functionality displayed at the molecule/air interface are important design principles for molecular electronic devices.

A common approach for making molecular electronic devices, such as molecular switch tunnel junctions (MSTJs) or rectifiers, is to sandwich a molecular film between two electrodes. Metal evaporation is often used to establish the top electrical contact in such devices. The interactions of evaporated metal with molecular films have been studied extensively,[1−14] and it has been shown that this step can potentially lead to device failure.[2,4,5,7−10] At one extreme, the metal reacts with and destroys or significantly alters the molecular layer. At the other extreme, the metal does not chemically react with the molecules but instead penetrates through the monolayer and electrically shorts the devices. Such problems are particularly important when the monolayer is composed of small molecules or the monolayer is loosely packed on the surface. A loosely packed monolayer is often characterized by molecules that are oriented at a large tilt angle with respect to the principal molecular axis and the surface normal, exposing much of the molecular structure to the incident flux of metal atoms. However, many groups have shown that, when the molecule/metal system is designed carefully and the molecular film is appropriately prepared, desired molecular functionality can survive the metal deposition process.[2−4,6,9,11] For example, the molecule might be designed to present specific functionality to the metal source, while protecting other key elements within the monolayer and preventing metal penetration through the molecular film. Examples include incorporation of a functional group at the monolayer/air interface that will react with a particular metal, such as CO_2CH_3 with Al[2] or thiols with Au or Al.[9] A second approach is to utilize a long or bulky sacrificial group that will react first with the impinging metal atoms.[6]

In this letter, we examine how the deposition of a top Ti electrode material affects the structure of Langmuir−Blodgett (LB) films[15,16] of a bistable [2]rotaxane molecular switch (Figure 1) and how it impacts the performance of MSTJ devices made from those monolayers. We carried out these investigations as a function of monolayer packing density. Three [2]rotaxane monolayers were prepared on an LB trough and compressed to different pressure values (and thus different packing densities) prior to transfer as LB films onto Pt or patterned poly-Si substrates. The monolayers on Pt substrates were characterized with Fourier transform reflection absorption infrared spectroscopy (FT-RAIRS), both before and after a 2 nm Ti overlayer was deposited. For the monolayers transferred onto patterned poly-Si substrates, MSTJ devices (using an identical 2 nm Ti adhesion layer for the top electrode) were fabricated and tested.

By varying the transfer pressure for rotaxane LB films, we were able to controllably vary the packing densities of the molecules on the surface. We demonstrated that the molecular film reacts differently with the Ti overlayer at different packing densities. These differences are reflected both in the RAIRS measurements and in the MSTJ device properties. At high packing densities (low area/molecule), the Ti appears to primarily react with the terminal groups, the tetraarylmethane hydrophobic stopper, whereas at low density, the Ti reacts less specifically, presumably over much of the length of the molecule.

Monolayers of an amphiphilic, bistable [2]rotaxane (Figure 1), were prepared on an LB trough (type 612D, Nima Technol-

* Corresponding author. E-mail: heath@caltech.edu.
[†] California Institute of Technology.
[‡] University of California.
[§] Current address: Department of Chemistry, Langston University, P.O. Box 907, Langston, OK 73050.

10.1021/jp0607723 CCC: $30.25

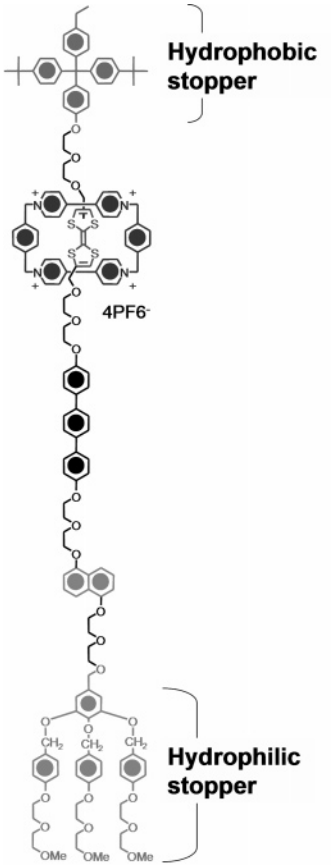

Figure 1. Structure of the redox-addressable, bistable [2]rotaxane molecular switch utilized in this study.

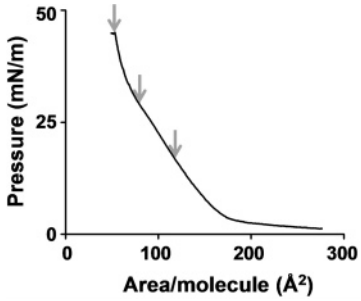

Figure 2. Pressure−area isotherm of the bistable [2]rotaxane. Arrows indicate transfer points along isotherm, which correspond to 15 mN/m (118 Å^2/molecule), 30 mN/m (73 Å^2/molecule), and 45 mN/m (54 Å^2/molecule).

ogy, Coventry, U.K.). An 80−100 μL volume of the molecule/chloroform solution (0.5 mg/mL) was applied to an aqueous (18 MΩ H_2O) subphase. Thirty minutes after deposition onto the water surface, the monolayer was compressed at a rate of 5 cm^2/min to the desired pressure. LB monolayers were transferred onto the Pt-coated wafers or onto patterned poly-Si substrates at a rate of 1 mm/min at transfer pressures of 15, 30, and 45 mN/m. These pressures translate to area/molecule values of 118, 73, and 54 Å^2, respectively (Figure 2). Prior to transfer, all monolayers were featureless via in situ Brewster angle microscopy. Contact angles were measured using a Ramé-Hart Inc. goniometer, model 100.

The FT-RAIR spectra were collected with a Bruker Vertex 70 FT-IR spectrometer, with p-polarized light at 80° or 85° incidence from the surface normal. IR radiation was detected using a liquid-nitrogen-cooled mercury cadmium telluride detector. For the bare monolayers, the background was taken from a blank silicon wafer coated with Ti/Pt. For the monolayer/Ti samples, the background was a silicon wafer coated with Ti/Pt and 2 nm Ti.

Fabrication of MSTJ devices has been described previously.[15,17−19] Briefly, bottom electrodes (1.5 μm wide) were patterned onto substrates of n-type poly-Si using photolithography. After cleaning with photoresist stripper (J. T. Baker Aleg-355) at 80 °C for 30 min, the substrates were rinsed thoroughly with 18 MΩ water and dried under a stream of nitrogen. The top electrode (30 μm wide, 2 nm Ti followed by 200 nm Al) was evaporated through a shadow mask.

The molecular superstructures of self-assembled monolayers of different bistable [2]rotaxanes on gold surfaces have been investigated through the use of theoretical modeling coupled with direct comparison with experiment.[20] Although those monolayers were on gold surfaces and the ones studied here are LB films on Pt or poly-Si, some observations from those studies are worth noting. The optimal packing density, as well as the surface tension, of these monolayers were calculated and shown to correlate well with experimental measurements of contact angles and film thicknesses. The thicknesses of the [2]-rotaxane monolayers in that study were found to be around 4 nm at the optimal packing density. The molecules were found to have tilt angles with respect to the surface normal of ∼40−45° (at 115 Å^2/molecule), depending on the [2]rotaxane structure. These tilt angles decreased (and the film thickness increased) with increasing packing density. In addition, as the area/molecule decreased, the contact angle increased, consistent with results of this study. Here, the measured contact angles were 65°, 81°, and 85°, corresponding to 118 Å^2/molecule, 73 Å^2/molecule, and 54 Å^2/molecule, respectively.

Table 1 summarizes the peak assignments for the FT-RAIRS data. In the following discussion of the FT-RAIRS, we have assumed that the spectral changes arise from chemical reactions between the Ti and the molecular film, and have ignored changes that may arise from changes in the selection rules. A large Ti oxide peak (870 cm^{-1}) was observed upon deposition of the 2 nm Ti film on both of the blank and the molecular monolayer substrates. Figure 3A shows the spectra for the monolayer transferred at 118 Å^2/molecule. The black traces show the IR spectra before Ti evaporation, and the gray after evaporation of 2 nm of Ti. The intensities of all the peaks decreased as compared to the higher-pressure cases (see below), due to the decreased coverage (larger area per molecule). The high-frequency region (Figure 3A left) shows the change that the Ti evaporation has on the C−H stretches of the molecule. The red trace (after Ti deposition) shows a large reduction (50−70%) of the C−H stretch of the $-CH_3$ groups (at 2966 and 2873 cm^{-1}) upon metal evaporation, indicating a reaction between the Ti and the $-CH_3$ groups of the molecule. The $-CH_3$ groups are at both ends of the molecule, but primarily in the hydrophobic stopper (see Figure 1). The low-frequency (Figure 3A right) region shows a large change after Ti deposition, indicating that much of the molecule has been affected by the Ti deposition. This observation is consistent with the large area per molecule (and corresponding high tilt angle). The molecules are neither upright nor tightly packed so that the bulky hydrophobic stopper offers little protection from the incident flux of metal atoms. However, these spectral changes do not necessarily indicate that the whole molecule is destroyed. Atomic force microscopy (AFM) studies of the formation of a Ti overlayer on alkanethiol self-assembled monolayers have shown that evaporated Ti forms clusters before forming a continuous film.[13] Thus, it is likely that the extent of the reaction between the molecule and the Ti varies from region to region.

TABLE 1: Peak Assignments for FT-RAIRS

	118 Å²/molecule		73 Å²/molecule		54 Å²/molecule	
assignment	bare ML	ML w/2 nm Ti	bare ML	ML w/2 nm Ti	bare ML	ML w/2 nm Ti
C−H stretch (−CH_3)	2966, 2873	2873 (shoulder)	2967, 2871	2964 (shoulder)	2966, 2873	2873
C−H stretch (−CH_2−)	2928, 2910	2930, 2859	2930, 2906	2930, 2859	2930, 2909	2930, 2859
C═C bend of phenyl rings	1608, 1507, 1493, 1457	none	1609, 1508, 1491, 1457	1608, 1508, 1492, 1457	1608, 1510, 1492, 1457	1608, 1510, 1492, 1457
C−O−C stretch	1250	1250	1252	1252	1250	1250

The next set of monolayers was transferred at 73 Å²/molecule. This pressure is the pressure that we have found optimal for preparing MSTJs from these and similar bistable [2]rotaxanes.[15,18,19] Thus, we expect a closely packed film. The RAIR spectra for the 73 Å²/molecule monolayer are shown in Figure 3B. Unlike the case for the 118 Å²/molecule monolayer, most of the low-frequency IR peaks are relatively unchanged by the deposition of the Ti. However, as with the case of the lower-pressure film, Ti deposition does significantly reduce the intensity of the −CH_3 peaks (at 2967 and 2871 cm^{-1}), indicating a reaction of the hydrophobic stopper with Ti. The right trace of Figure 3B shows a reduction in the 1508 cm^{-1} peak after Ti deposition. This peak corresponds to the C═C bends of the phenyl rings, a large number of which are in the hydrophobic stopper. This reduction in intensity provides further evidence of the reaction of the Ti metal with the hydrophobic stopper. The other peaks have similar relative intensities before and after deposition.

In Figure 3C, we present the spectra for the monolayer transferred at 54 Å²/molecule. The results are similar to the 73 Å²/molecule case: Only a few peaks are significantly affected by the Ti deposition. The most notable changes again are the reduction of the peaks at 2966, 2873 (C−H stretch of −CH_3), and 1510 cm^{-1} (C═C bend of phenyl groups).

The spectroscopic data provides a more complete story when correlated with MSTJ device performance characteristics. The pressure at which the monolayer is transferred and the damage to the monolayer that accompanies Ti deposition should both strongly influence the device characteristics. Devices were made at each of the three areas per molecule (118, 73, and 54 Å²/molecule). For all devices, measurements of current−voltage traces, remnant molecular signature plots,[17] and switch cycling between on and off states were measured. Some of these data are presented in Figure 4.

Although there was device-to-device variation in the current levels, the highest current level was generally observed in the 118 Å²/molecule devices, followed by the 73 Å²/molecule devices and then the 54 Å²/molecule. This observation is not surprising if one considers the increasing thickness of the LB film that accompanies increasing transfer pressure. The remnant molecular signature data reveals the capacitance-free, hysteretic current−voltage response of an MSTJ, and these data are presented for each transfer pressure in Figure 4A.[21] These plots also reveal the magnitude of the switching amplitude (on/off ratio). The 118 Å²/molecule device showed no clear hysteresis. The remnant molecular signature for the 73 Å²/molecule device is typical for this molecule and reveals an on/off ratio of 10:1.

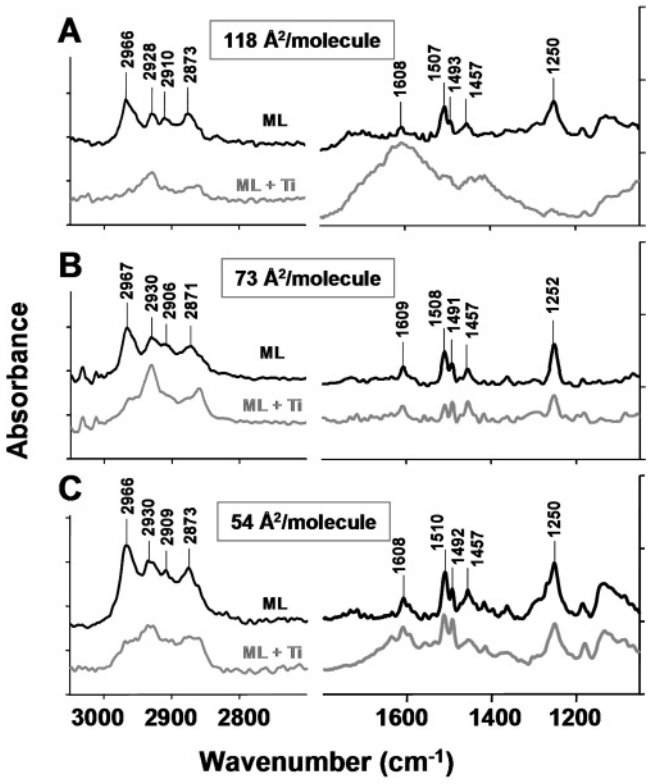

Figure 3. RAIR spectra of the [2]rotaxane monolayers (ML) before and after deposition of 2 nm Ti. (A) 15 mN/m (118 Å²/molecule) transfer pressure. (B) 30 mN/m (73 Å²/molecule) transfer pressure. (C) 45 mN/m (54 Å²/molecule) transfer pressure. Left-hand *y*-axis scale (3050−2700 cm^{-1} region): Each tick corresponds to 0.001 absorbance unit. Right-hand *y*-axis scale (1800−1050 cm^{-1} region): Each tick corresponds to 0.005 absorbance unit.

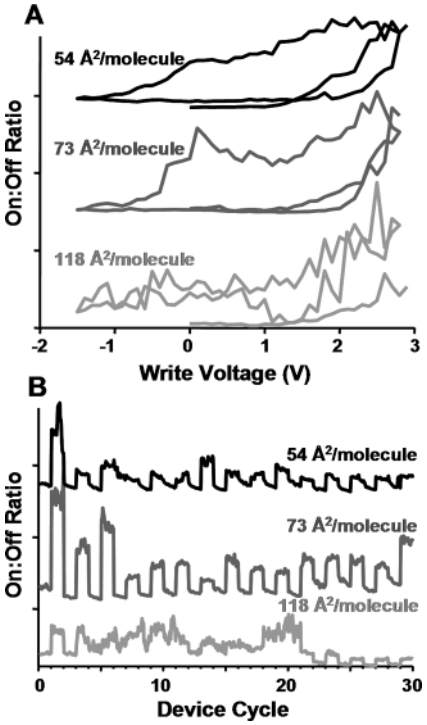

Figure 4. (A) Remnant hysteresis plots for MSTJ devices at 54, 73, and 118 Å²/molecule. (B) Device cycling data. The two devices that were prepared at the higher packing densities exhibit approximately the same switching amplitude in both the remnant (10:1) and the cycling (3:1) data, although the current magnitude for the 54 Å²/molecule MSTJ is significantly less than for the 73 Å²/molecule MSTJ.

For the 54 Å^2/molecule, the current magnitude compared to the 73 Å^2/molecule device is decreased, but the on/off ratio is still approximately 10:1.

In Figure 4B, we present switch cycling data for the MSTJs prepared at the three different pressures.[22] The 118 Å^2/molecule device exhibits erratic behavior with little or no hysteresis: This was typical of all the junctions prepared at this area/molecule. All 73 Å^2/molecule devices exhibited cycling behavior. The data in Figure 4B show 30 switching cycles from an MSTJ that exhibited an on/off ratio, in this measurement mode, of at least 3:1 for every cycle. The 54 Å^2/molecule devices also cycled, although they were not as easy to "turn off" as the 73 Å^2/molecule device. We have recently thoroughly investigated the effect of physical environment on the temperature-dependent switching kinetics[23−25] and bistability thermodynamics[19] of both [2]rotaxanes and [2]catenanes and found that more sterically restricted molecules exhibited higher energy barriers for relaxation from the switch-closed (metastable) state to the switch-open (ground) state. Thus, it is likely that the increased packing within the LB films for the 54 Å^2/molecule monolayers is reflected in a larger activation barrier to switching.

The correlation of the FT-RAIRS data with the device performance data is revealing. First, it does appear that, under certain conditions, molecular monolayers of bistable [2]rotaxanes can be largely protected from the deposition of a top Ti electrode material. The FT-RAIRS data is consistent with the Ti reacting top-down with the molecular monolayer, and with the bulky hydrophobic stopper serving to protect the key switching elements of the molecule. Unfortunately, from the IR spectroscopic data, it is not possible to individually assign each of the molecular functional groups to an individual spectroscopic peak. However, when the RAIRS data is coupled to device performance metrics, it is reasonable to assume that the Ti reacts primarily with the terminal hydrophobic stoppers. For the cases of the higher-pressure (73 and 54 Å^2/molecule) devices, robust device performance is observed, although the highest-pressure devices exhibit evidence that the tight packing of the monolayer is reducing the switching kinetic rates. These results indicate that methods for MSTJ device fabrication, as well as the metrics for MSTJ device performance, depend greatly upon the structure of the molecular monolayer that ends up sandwiched between the two electrodes. This situation is consistent with other work in the field, and thus may imply that these observations are general for molecular electronic devices.

Acknowledgment. This work was funded by the DARPA MolApps Program and by the MARCO Center for Materials, Structures and Devices. D.D.H. acknowledges Caltech's MURF program.

References and Notes

(1) Jung, D. R.; Czanderna, A. W. *Crit. Rev. Solid State Mater. Sci*. **1994**, *19*, 1−54.

(2) Hooper, A.; Fisher, G. L.; Konstadinidis, K.; Jung, D.; Nguyen, H.; Opila, R.; Collins, R. W.; Winograd, N.; Allara, D. L. *J. Am. Chem. Soc*. **1999**, *121*, 8052−8064.

(3) Fisher, G. L.; Hooper, A. E.; Opila, R. L.; Allara, D. L.; Winograd, N. *J. Phys. Chem. B* **2000**, *104*, 3267−3273.

(4) Fisher, G. L.; Walker, A. V.; Hooper, A. E.; Tighe, T. B.; Bahnck, K. B.; Skriba, H. T.; Reinard, M. D.; Haynie, B. C.; Opila, R. L.; Winograd, N.; Allara, D. L. *J. Am. Chem. Soc*. **2002**, *124*, 5528−5541.

(5) Walker, A. V.; Tighe, T. B.; Reinard, M. D.; Haynie, B. C.; Allara, D. L.; Winograd, N. *Chem. Phys. Lett*. **2003**, *369*, 615−620.

(6) Chang, S.-C.; Li, Z.; Lau, C. N.; Larade, B.; Williams, R. S. *Appl. Phys. Lett*. **2003**, *83*, 3198−3200.

(7) Walker, A. V.; Tighe, T. B.; Carbarcos, O. M.; Reinard, M. D.; Haynie, B. C.; Uppilli, S.; Winograd, N.; Allara, D. L. *J. Am. Chem. Soc*. **2004**, *126*, 3954−3963.

(8) Walker, A. V.; Tighe, T. B.; Stapleton, J.; Haynie, B. C.; Uppilli, S.; Allara, D. L.; Winograd, N. *Appl. Phys. Lett*. **2004**, *84*, 4008−4010.

(9) de Boer, B.; Frank, M. M.; Chabal, Y. J.; Jiang, W.; Garfunkel, E.; Bao, Z. *Langmuir* **2004**, *20*, 1539−1542.

(10) Tai, Y.; Shaporenko, A.; Eck, W.; Grunze, M.; Zharnikov, M. *Appl. Phys. Lett*. **2004**, *85*, 6257−6259.

(11) Nowak, M. A.; McCreery, R. L. *Anal. Chem*. **2004**, *76*, 1089−1097.

(12) Walker, A. V.; Tighe, T. B.; Haynie, B. C.; Uppilli, S.; Winograd, N.; Allara, D. L. *J. Phys. Chem. B* **2005**, *109*, 11263−11272.

(13) Tighe, T. B.; Daniel, T. A.; Zhu, Z.; Winograd, N.; Allara, D. L. *J. Phys. Chem. B* **2005**, *109*, 21006−21014.

(14) Wagner, A. J.; Wolfe, G. M.; Fairbrother, D. H. *Appl. Surf. Sci*. **2003**, *219*, 317−328.

(15) Collier, C. P.; Jeppesen, J. O.; Luo, Y.; Perkins, J.; Wong, E. W.; Heath, J. R.; Stoddart, J. F. *J. Am. Chem. Soc*. **2001**, *123*, 12632−12641.

(16) Lee, I. C.; Frank, C. W.; Yamamoto, T.; Tseng, H.-R.; Flood, A. H.; Stoddart, J. F.; Jeppesen, J. O. *Langmuir* **2004**, *20*, 5809−5828.

(17) Collier, C. P.; Mattersteig, G.; Luo, Y.; Wong, E. W.; Beverly, K.; Sampaio, J.; Raymo, F.; Stoddart, J. F.; Heath, J. R. *Science* **2000**, *289*, 1172−1175.

(18) Luo, Y.; Collier, C. P.; Jeppesen, J. O.; Nielsen, K. A.; DeIonno, E.; Ho, G.; Perkins, J.; Tseng, H.-R.; Yamamoto, T.; Stoddart, J. F.; Heath, J. R. Two-dimensional molecular electronics circuits. *ChemPhysChem* **2002**, *3*, 519−525.

(19) Choi, J. W.; Flood, A. H.; Steuerman, D. W.; Nygaard, S.; Braunschweig, A. B.; Moonen, N. N. P.; Laursen, B. W.; Luo, Y.; DeIonno, E.; Peters, A. J.; Jeppesen, J. O.; Xu, K.; Stoddart, J. F.; Heath, J. R.. *Chem.—Eur. J*. **2006**, *12*, 261−279.

(20) (a) Jang, S. S.; Jang, Y. H.; Kim, Y. H.; Goddard, W. A., III; Choi, J. W.; Heath, J. R.; Laursen, B. W.; Flood, A. H.; Stoddard, J. F.; Norgaard, K.; Bjornholm, T. *J. Am Chem. Soc*. **2005**, *127*, 14804−14816. (b) Jang, S. S.; Jang, Y. H.; Kim, Y. H.; Goddard, W. A., III; Flood, A. H.; Laursen, B. W.; Tseng, H. R.; Stoddart, J. F.; Jeppesen, J. O.; Choi, J. W.; Steuerman, D. W.; DeIonno, E.; Heath, J. R. *J. Am. Chem. Soc*. **2005**, *127*, 1563−1575.

(21) The remnant molecular signature was measured by varying the write voltage in 100 mV steps from 0 to 2.8, to −1.5, to 3.0 V, and reading at 250 mV after each write pulse. Plotted is the write voltage vs the current at the reading bias.

(22) The device cycling data was generated by reading at a bias of +0.25 V, as the device was alternately closed at +2.8 V and opened at −1.5 V.

(23) Steuerman, D. W.; Tseng, H.-R.; Peters, A. J.; Flood, A. H.; Jeppesen, J. O.; Nielsen, K. A.; Stoddart, J. F.; Heath, J. R. *Angew. Chem., Int. Ed*. **2004**, *43*, 2−7.

(24) Flood, A. H.; Peters, A. J.; Vignon, S. A.; Steuerman, D. W.; Tseng, H.-R.; Kang, S.; Heath, J. R.; Stoddart, J. F. *Chem.—Eur. J*. **2004**, *10*, 6558−6564.

(25) Flood, A. H.; Stoddart, J. F.; Steuerman, D. W.; Heath, J. R. *Science* **2004**, *306*, 2055−2056.